A. S. Ledkov, R. S. Pikalov, Nonlinear Control of Tether Retrieval in an Elliptical Orbit, *Rus. J. Nonlin. Dyn.*, 2023, том 19, номер 2, 201–218

DOI: 10.20537/nd230401

Russian Journal of Nonlinear Dynamics, 2023, vol. 19, no. 2, pp. 201–218.
Full-texts are available at http://nd.ics.org.ru
DOI: 10.20537/nd230401

NONLINEAR PHYSICS AND MECHANICS

MSC 2010: 70Q05

Nonlinear Control of Tether Retrieval in an Elliptical Orbit

A. S. Ledkov, R. S. Pikalov

Tether retrieval is an important stage in many projects using space tether systems. It is known that uniform retrieval is an unstable process that leads to the winding of the tether on a satellite at the final stage of retraction. This is a serious obstacle to the practical application of space tethers in the tasks of climbing payloads to a satellite and docking the spacecraft with a tethered satellite after its capture. The paper investigates the plane motion of a space tether system with a massless tether of variable length in an elliptical orbit. A new control law that ensures the retrieval of the tether without increasing the amplitude of oscillations at the final stage is proposed. The asymptotic stability of the space tether system's controlled motion in an elliptical orbit is proved. A numerical analysis of tether retrieval is carried out. The influence of the eccentricity of the orbit on the retrieval process is investigated. The results of the work can be useful in preparing missions of the active space debris removal and in performing operations involving tether retrieval.

Keywords: space tether system, retrieval, nonlinear, control law, tether

1. Introduction

Space tether systems can be used to solve a wide class of problems of modern and future astronautics. They are able to take astronautics to a new level by solving a number of important practical tasks: reentry payloads from space station, creation of artificial gravitation, control of the joint motion of connected objects, changing orbits and implementation of transport operations, capture and removal of space debris objects, extractions of minerals and exploration of

Received November 29, 2022
Accepted March 20, 2023

This study was supported by the Russian Science Foundation (Project No. 19-19-00085).

Alexander S. Ledkov
ledkov@inbox.ru
Ruslan S. Pikalov
pickalovrs@gmail.com
Samara National Research University
ul. Moskovskoye shosse 34, Samara, 443086 Russia

asteroids, planetoids and satellites [1, 2]. Many projects of tethered space systems involve the use of a variable length tether. In particular, the task of reentry payloads from a space station assumes that there is a space tether system in orbit [3, 4]. The payload is docked to the lower tip of the tether, after that the tether is retrieved into the satellite. This scheme of transportation saves fuel [5]. The space debris removal is another important task, where a variable-length tether can be used. One of the possible schemes involves the tether capture of space debris, after which the tether is retracted and provides a safe docking of the spacecraft with the space debris object [6]. After docking, the spacecraft and space debris move as a single unit. The tethered capture can be carried out using a probe-cone device [7], telescopic robotic arm [8], harpoon [9] or space net [10].

Instability of tether oscillations is the main difficulty in implementing the tether retrieval process. When the tether is retracted at a constant speed, the tether is wound onto the satellite, which can lead to satellite breakdown, tether rupture and collision of the satellite with a subsatellite attached to the tether. The issue of developing tether control laws and methods for safe and efficient retraction is an urgent task that requires a detailed study and solution. A large number of studies are concerned with this problem. Ref. [3] provides an overview of existing research devoted to modeling and analyzing the dynamics of space tether systems in the deployment and retrieval mode, as well as various laws and methods of controlling the space tether system in these motion modes. A detailed overview of control laws for tethered systems is also given in [4]. The use of additional engines on a tethered subsatellite greatly simplifies the task. Combined control schemes based on the control of the tether retrieval velocity and the engines thrust are proposed in [11–13]. Special attention is given in the literature to retrieving the tether by controlling the tension force, retraction velocity, or length of the tether.

In [14] and [15], a law of tether retrieval based on the calculation of the "mission function" is proposed. The application of linear laws of tension force control is considered in [16] and [17]. In [18], a family of tether length control laws is considered, for which analytical solutions are obtained for the angles of deviation of the tether from the local vertical and from the plane of the orbit. The results of the study are developed in [19]. The fractional order control theory was used in [20] to develop a fast and stable law of tether retraction.

In [21], the relay law of tether retraction is considered, when the folding mechanism can provide either zero or constant tether retraction velocity. In [22], a three-parameter law for controlling the tension force of the tether is developed. This control law ensures the retraction of the tether without rotating the system at the final stage. It is shown that, in contrast to deployment, where stable motion can be provided by a two-parameter control law (for example, [23]), a three-parameter control law of the tether tension force is necessary for stable retraction. A trigonometric law in the form of a power series satisfying boundary conditions for controlling the length of the tether is considered in [24]. Ref. [25] discusses the use of the feedback control law of the tether tension force. The control law is used for simulating the processes of tether deployment and retraction in the case of a circular orbit using a hinge-rod model of the tether, taking into account the influence of the atmosphere. An alternative law of the tether tension force is proposed in [26], where the retrieving process is divided into two stages. In [27], an original control scheme based on the calculation of the energy of the tether system is proposed, which provides stabilization of the angular oscillations of the tether during retrieval. The asymptotic stability of the control law is proved using the Lyapunov function and LaSalle's invariance principle. In [28], the tether tension control law is proposed. The asymptotic stability is proved using the Lyapunov theory. An alternative law for the case of spatial motion is proposed in [29]. In [30], a law of tether deployment and retrieval based on the full-order sliding

mode tension control scheme is developed, taking into account the requirement of positivity for the tether tension force. The control law for the deployment and retraction of the tether based on the calculation of the energy of the system is proposed in [31].

Many researchers have tried to develop optimal control laws for tether retrieval using various approaches and optimality criteria. In [32–36], optimal trajectories of motion of the subsatellite during tether retrieval processes are constructed while solving various tasks: minimum tension force [33], performance [34, 35] or damping of tether oscillations in the plane of a circular orbit [36]. Nonlinear receding horizon control was developed in [37] for the case of deploying and retracting a tether system. The proposed algorithm overcomes numerical difficulties associated with the tendency to infinity of the penalty function.

All the results described above were obtained for the partial case of a circular orbit, which is quite rare in practice. The behavior of a space tether system in an elliptical orbit is much more complex. There is a possibility of occurrence of resonances and chaotic modes of motion [41]. The dynamics of the controlled motion of a space tether system in a Keplerian orbit is studied in [42]. Ref. [40] is devoted to the study of the dynamics of a space tether system of variable length in an elliptical orbit, where the exponential law of change in the tether length is used and an analysis of the topology of the phase space of the dumbbell tether model is carried out. Sliding mode control is used in [43] to perform tether deployment in low-eccentricity orbits. The optimal trajectories for the deployment and retrieval of a space tether system in an elliptical orbit are obtained in [38]. The study [39] analyzes the impact of perturbing factors of the space environment for a variable length tether mission.

An analysis of the literature has shown that the issue of developing control laws for tether retrieval is quite well developed for the case of a circular orbit, but for an elliptical orbit it is poorly studied. The aim of this study is to develop a control law that ensures the retrieval of the space tether system without increasing the angle of the tether deviation from the local vertical at the final stage of the tether retraction process in the case of the system motion in an elliptical orbit.

2. Mathematical model

2.1. Equations of motion

Consider a mechanical system shown in Fig. 1. In this study it is assumed that the tether is an elastic and weightless rod. The satellite and the subsatellite are considered as material points connected by a tether. It is assumed that the tether system oscillates in the plane of the orbit.

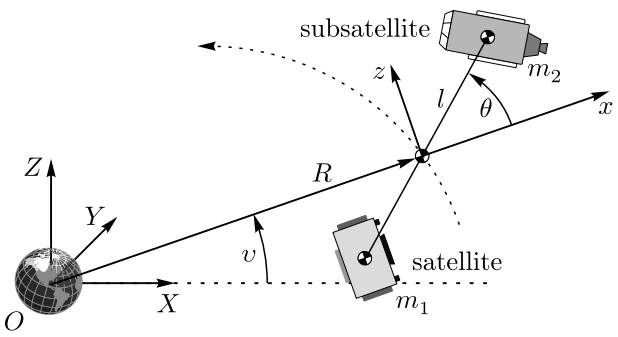

Fig. 1. Scheme of the system and generalized coordinates

The motion of the system can be described by the following generalized coordinates: θ is the angle of declination of a tether from the tangent to the orbit of the center of mass of a tethered system, and the relative tether length $\Lambda = \frac{l}{l_0}$, where l is the tether length and l_0 is the initial tether length. A detailed description of how the equations are obtained is given in [38]. Let us use Eqs. (27) and (29) from [38] under the following assumptions: the tether's out-of-plane deflection angle is zero ($\varphi \equiv 0$), the mass of the tether is negligible compared to the mass of the bodies connected by it ($m_t = 0$), and motion occurs only under the influence of gravitational forces ($\Theta_\theta = 0$). In this case the equation of motion can be written as

$$\theta'' = 2(\theta' + 1)\left[\frac{e\sin\nu}{\kappa} - \frac{\Lambda'}{\Lambda}\right] - \frac{3}{\kappa}\sin\theta\cos\theta, \tag{2.1}$$

$$\Lambda'' = \frac{2e\sin\nu}{\kappa}\Lambda' + \Lambda\left[(\theta' + 1)^2 + \frac{1}{\kappa}\left(3\cos^2\theta - 1\right)\right] - \frac{Tmp^3}{m_1 m_2 l_0 \mu\kappa^4}. \tag{2.2}$$

where $\kappa = 1 + e\cos\nu$, L_r is the length of the unreformed tether, T is the tether tension force, ν is the orbit true anomaly, μ is the gravitational parameter of the Earth, p is the semi-latus rectum, e is the orbit eccentricity, and $()' = \frac{d}{d\nu}$.

2.2. The law of control

To find the control law for the tether length, which ensures the tether retraction at a constant angle θ, let us introduce the control parameter

$$u = \frac{\Lambda'}{\Lambda} \tag{2.3}$$

and substitute it, as well as the expression $\theta' = 0$, $\theta'' = 0$, into Eq. (2.1)

$$0 = 2\left[\frac{e\sin\nu}{\kappa} - u\right] - \frac{3}{\kappa}\sin\theta\cos\theta.$$

Expressing u gives

$$u = \frac{e\sin\nu}{1 + e\cos v} - \frac{3\sin 2\theta}{4(1 + e\cos v)}. \tag{2.4}$$

Substituting (2.4) into (2.3) allows us to write the control law for tether retraction velocity, which provides a constant angle θ

$$\Lambda' = \frac{1}{1 + e\cos v}\left(e\sin\nu - \frac{3}{4}\sin 2\theta\right)\Lambda. \tag{2.5}$$

Obviously, the minimum negative value of Λ' , corresponding to the fastest retraction of the tether, is reached when $\theta_* = \frac{\pi}{4}$.

In order to transfer the tether system from the initial position θ_0, θ_0' to the angular position $\theta_* = \frac{\pi}{4}$, $\theta_*' = 0$ corresponding to the fastest retraction, the feedback control terms are added in (2.4)

$$u = \frac{e\sin\nu}{1 + e\cos v} - \frac{3\sin 2\theta}{4(1 + e\cos v)} + \frac{k_1\theta'}{2} + \frac{k_2}{2}(\theta - \theta_*) + \frac{3\theta'}{4(1 + e\cos v)}, \tag{2.6}$$

where k_1 and k_2 are the control coefficients. As the angular position $\theta_* = \frac{\pi}{4}$, $\theta_*' = 0$ is reached, the influence of the third and fourth terms in expression (2.6) decreases, and the retrieval proceeds

according to a law close to (2.5). The addition term $\frac{3\theta'}{4(1+e\cos v)}$ is also added to the control law. The presence of this term greatly simplifies the subsequent analysis of the stability of the system motion.

Substituting (2.6) into (2.1) taking into account (2.3) gives a system of equations describing the controlled motion of the considered tethered system

$$\theta'' = 2(\theta'+1)\left[\frac{3\sin 2\theta}{4(1+e\cos v)} - \left(\frac{k_1}{2}+\frac{3}{4(1+e\cos v)}\right)\theta' - \frac{k_2}{2}(\theta-\theta_*)\right] - \frac{3\sin\theta\cos\theta}{1+e\cos v}, \quad (2.7)$$

$$\Lambda' = \left(\frac{e\sin\nu}{1+e\cos v} - \frac{3}{4(1+e\cos v)}\sin 2\theta + \left(\frac{k_1}{2}+\frac{3}{4(1+e\cos v)}\right)\theta' + \frac{k_2}{2}(\theta-\theta_*)\right)\Lambda. \quad (2.8)$$

This system of equations (2.7), (2.8) belongs to the class of nonlinear systems of differential equations with periodic coefficients. In the next section it will be proved that the equilibrium position $\theta = \theta_* = \frac{\pi}{4}$, $\theta' = 0$, $\Lambda = 0$ is asymptotically stable.

The system obtained describes the motion of two material points connected by an elastic massless rod. This means that a situation is possible where the tension force in the rod becomes negative as a result of using the control (2.6). In the case of a tether system, this will be expressed in slacking of the tether, and Eqs. (2.7) and (2.8) will no longer correctly describe the motion of the tether system. To control this situation, it is necessary to monitor the value of the tension force, which can be expressed from Eq. (2.2)

$$T = \left(\frac{2e\sin\nu}{\kappa}\Lambda' + \Lambda\left[(\theta'+1)^2 + \frac{1}{\kappa}\left(3\cos^2\theta - 1\right)\right] - \Lambda''\right)\frac{m_1 m_2 l_0 \mu\kappa^4}{mp^3}. \quad (2.9)$$

The second derivative Λ'' included in this expression can be found by differentiating expression (2.8)

$$\Lambda'' = \left(\frac{1}{1+e\cos v}\left(e\sin\nu - \frac{3}{4}\sin 2\theta\right) + \left(\frac{k_1}{2}+\frac{3}{4(1+e\cos v)}\right)\theta' + \frac{k_2}{2}(\theta-\theta_*)\right)\Lambda' +$$
$$+\left[\frac{1}{1+e\cos v}\left(e\cos\nu - \frac{3}{2}\cos(2\theta)\theta'\right) + \frac{1}{(1+e\cos v)^2}\left(e^2\sin^2\nu - \frac{3}{4}e\sin\nu\sin 2\theta + \frac{3}{4}e\theta'\sin\nu\right) +\right.$$
$$\left. + \left(\frac{k_1}{2}+\frac{3}{4(1+e\cos\nu)}\right)\theta'' + \frac{k_2}{2}\theta'\right]\Lambda. \quad (2.10)$$

Substituting (2.8) and (2.10) into (2.9) allows us to define the value of the tether tension force T.

2.3. Study of the stability of controlled motion

To study the stability of periodic motions of a nonlinear system of equations with periodic coefficients, one can use Lyapunov's theorem on stability in the first approximation [44]. The change of variables

$$x_1 = \Lambda, \quad x_2 = \theta - \frac{\pi}{4}, \quad x_3 = \theta' \quad (2.11)$$

allows us to rewrite the system (2.7)–(2.8) in the form

$$x_1' = \frac{ex_1\sin v}{1+e\cos v} - \frac{3x_1\cos(2x_2)}{4(1+e\cos v)} + \left(\frac{k_1}{2}+\frac{3}{4(1+e\cos v)}\right)x_1x_3 + \frac{k_2x_1x_2}{2},$$
$$x_2' = x_3, \quad (2.12)$$
$$x_3' = \frac{3x_3(\cos 2x_2 - x_3 - 1)}{2(1+e\cos v)} - (x_3+1)[k_1x_3 + k_2x_2].$$

The right-hand side of the system of equations (2.12) can be expanded as the Maclaurin series

$$\begin{gathered} x_1' = \left(\frac{4e\sin v - 3}{4(1+e\cos v)}\right) x_1 + X_1(v,\, x_1,\, x_2,\, x_3), \\ x_2' = x_3, \\ x_3' = -k_2 x_2 - k_1 x_3 + X_3(v,\, x_1,\, x_2,\, x_3), \end{gathered} \tag{2.13}$$

where the nonlinear part X_1, X_3 has the form

$$X_1(v,\, x_1,\, x_2,\, x_3) = \left(\frac{k_1}{2} + \frac{3}{4(1+e\cos v)}\right) x_1 x_3 + \frac{k_2 x_1 x_2}{2} + \frac{3x_3}{2(1+e\cos v)} \sum_{j=2}^{\infty} \frac{(-1)^{j-1}(2x_2)^{2j-2}}{(2j-2)!},$$

$$X_3(v,\, x_1,\, x_2,\, x_3) = \frac{3x_3}{2(1+e\cos v)} \sum_{j=2}^{\infty} \frac{(-1)^{j-1}(2x_2)^{2j-2}}{(2j-2)!} - \left(\frac{k_1}{2} + \frac{3}{4(1+e\cos v)}\right) x_3^2 - k_2 x_2 x_3.$$

The presence of the last term in the control law (2.6) leads to the absence of the term $\frac{3x_3}{2+2e\cos v}$ in the linear part of the equation x_3'. The equations of the first approximation have the form

$$\begin{gathered} x_1' = \left(\frac{4e\sin v - 3}{4(1+e\cos v)}\right) x_1, \\ x_2' = x_3, \\ x_3' = -k_2 x_2 - k_1 x_3. \end{gathered} \tag{2.14}$$

According to Lyapunov's first approximation stability theorem for a system of nonlinear equations with periodic coefficients, if all the roots of the characteristic equation of the first approximation (2.14) have absolute values smaller than one, then the undisturbed motion is asymptotically stable, and if there is at least one root with an absolute value greater than one, then the undisturbed motion is unstable [44]. To apply this theorem, the existence of a domain $v > v_0$, $|x_i| < H$, in which inequalities are satisfied $|X_i(v,\, x_1,\, x_2,\, x_3)| \leqslant A(|x_1| + |x_2| + |x_3|)$ is necessary. If this condition is not met, the behavior of systems (2.15) and (2.14) in the vicinity of the equilibrium position may differ qualitatively. For the considered system of equations, taking into account that $x_1 < 1$ and $\sum\limits_{j=2}^{\infty} \frac{(-1)^{j-1}(2x_2)^{2j-2}}{(2j-2)!} = \cos(2x_2) - 1$, it can be written

$$\begin{gathered} |X_1(v,\, x_1,\, x_2,\, x_3)| \leqslant \left(\frac{k_1}{2} + \frac{3}{4(1-e)}\right) H^2 + \frac{k_2 H^2}{2} = A_1 = \text{const}, \\ |X_3(v,\, x_1,\, x_2,\, x_3)| \leqslant \frac{3H}{(1-e)} + \left(\frac{k_1}{2} + \frac{3}{4(1-e)}\right) H^2 + k_2 H^2 = A_2 = \text{const}. \end{gathered} \tag{2.15}$$

These estimates are valid for the parameters $k_1 \geqslant 0$, $k_2 \geqslant 0$.

A fundamental system of solutions for Eqs. (2.14) is required to obtain the characteristic equation. The system (2.14) can be integrated analytically:

$$x_1 = -C_1 \kappa^{-1} \exp\left(\frac{3}{2\sqrt{\kappa}} \arctan\left(\frac{1-e}{\sqrt{1-e^2}} \tan\frac{v}{2}\right)\right), \tag{2.16}$$

$$x_2 = C_2 \exp(p_1 v) + C_3 \exp(p_2 v), \tag{2.17}$$

$$x_3 = C_2 p_1 \exp(p_1 v) + C_3 p_2 \exp(p_2 v), \tag{2.18}$$

where $p_1 = \frac{-k_1+\sqrt{k_1^2-4k_2}}{2}$, $p_2 = \frac{-k_1-\sqrt{k_1^2-4k_2}}{2}$. The solution has a gap at points $v = 2\pi j + \pi$, where $j \in \mathbb{Z}$. At these points, the tangent tends to infinity, and when $v \to (2\pi j + \pi) - 0$ we have $\tan\frac{v}{2} \to +\infty$ and $\arctan(\infty) = \frac{\pi}{2}$, and when $v \to (2\pi j + \pi) + 0$ we have $\tan\frac{v}{2} \to -\infty$ and $\arctan(-\infty) = -\frac{\pi}{2}$. To get rid of the gap, let us multiply the solution (2.16) by the coefficient $f(v)$ and make it so that $x_1((2\pi j + \pi) - 0) = x_2((2\pi j + \pi) + 0)f(v)$. This equality holds if $f(v) = \exp\left(-\frac{3\pi}{2\sqrt{1-e^2}}\operatorname{floor}\left(\frac{v+\pi}{2\pi}\right)\right)$. Thus, the solution for x_1 takes the form

$$x_1 = -C_1\kappa^{-1}\exp\left(-\frac{3}{2\sqrt{\kappa}}\left(\arctan\left(\frac{1-e}{\sqrt{1-e^2}}\tan\frac{v}{2}\right) + \pi\operatorname{floor}\left(\frac{v+\pi}{2\pi}\right)\right)\right). \tag{2.19}$$

Taking into account (2.17)–(2.19), the matrix of the fundamental system of solutions can be written in the form

$$\mathbf{\Phi} = \begin{bmatrix} \kappa^{-1}\exp\left(\frac{-3}{2\sqrt{\kappa}}\left(\arctan\left(\frac{1-e}{\sqrt{1-e^2}}\tan\frac{v}{2}\right) + \pi\operatorname{floor}\left(\frac{v+\pi}{2\pi}\right)\right)\right) & 0 & 0 \\ 0 & \exp(p_1 v) & \exp(p_2 v) \\ 0 & p_1\exp(p_1 v) & p_2\exp(p_2 v) \end{bmatrix}. \tag{2.20}$$

Each column of this matrix $\mathbf{X}_i(v)$ represents a linearly independent solution of the system (2.14). Since the coefficients on the right-hand sides of the system of equations are 2π-periodic functions, it is possible to write the matrix equation $\mathbf{\Phi}(v + 2\pi) = \mathbf{A}\mathbf{\Phi}(v)$, which allows us to find the matrix $\mathbf{A} = \mathbf{\Phi}(v + 2\pi)\mathbf{\Phi}(v)^{-1}$. Then the characteristic equation corresponding to the period 2π for a system of linear equations with periodic coefficients has the form [44]

$$D(\rho) = \det(\mathbf{A} - \rho\mathbf{E}) = 0, \tag{2.21}$$

where $\mathbf{E}$ is the unit matrix and ρ is the root of the characteristic equation.

For the considered system of the first approximation, Eq. (2.21) gives the following roots of the characteristic equation:

$$\rho_1 = \exp\left(-\frac{3\sqrt{1-e^2}}{2(1-e^2)}\right), \quad \rho_2 = \exp(2\pi p_1), \quad \rho_3 = \exp(2\pi p_2). \tag{2.22}$$

The root $\rho_1 < 1$ for any of $e < 1$. Consider the remaining roots. In the case $k_2 \leqslant \frac{k_1^2}{4}$, the variables p_1 and p_2 are real numbers, and for the absolute values of the second and third roots of the characteristic equation to be less than one, the following inequalities must be satisfied:

$$p_1 = \frac{-k_1 + \sqrt{k_1^2 - 4k_2}}{2} < 0, \quad p_2 = \frac{-k_1 - \sqrt{k_1^2 - 4k_2}}{2} < 0. \tag{2.23}$$

The first inequality holds in the area ($k_1 > 0$, $k_2 > 0$), and the second in the area $\left(k_1 > 0,\ k_2 \leqslant \frac{k_1^2}{4}\right) \cup (k_1 \leqslant 0,\ k_2 < 0)$. The intersection of these areas is $\left(k_1 > 0,\ 0 < k_2 \leqslant \frac{k_1^2}{4}\right)$.

In the case $k_2 > \frac{k_1^2}{4}$, the variables p_1 and p_2 are complex numbers, and $p_{1,2} = \frac{-k_1}{2} \pm i\frac{\sqrt{4k_2-k_1^2}}{2}$. In this case, the roots of the characteristic equation can be rewritten using Euler 's formula:

$$\rho_{2,3} = \exp(-\pi k_1)\exp\left(\pm i\pi\sqrt{4k_2 - k_1^2}\right) = \\ = \exp(-\pi k_1)\left(\cos\left(\pi\sqrt{4k_2 - k_1^2}\right) \pm i\sin\left(\pi\sqrt{4k_2 - k_1^2}\right)\right),$$

the absolute value of these roots is $|\rho_{2,3}| = \exp(-\pi k_1)$. It is less than one when $k_1 > 0$.

Combining the case of complex and real roots, we find that $|\rho_2| < 1$ and $|\rho_3| < 1$ when $k_1 > 0$, $k_2 > 0$. In this case, the controlled motion in an elliptical orbit is asymptotically stable.

3. Results of numerical simulations

To confirm the effectiveness of the proposed control law (2.6), let us conduct a series of numerical simulations using the system of equations (2.7), (2.8). The parameters of the mechanical system considered are specified in Table 1. At the initial time $\nu_0 = 0$ the system has the following initial conditions:

$$\theta_0 = 0, \quad \theta_0' = 0, \quad \Lambda_0 = 1.$$

According to (2.3), these initial conditions correspond to the initial value of the relative tether length derivative

$$\Lambda_0' = \frac{e \sin \nu_0}{1 + e \cos v_0} - \frac{k_2 \theta_*}{2}, \tag{3.1}$$

and the initial velocity of the tether retraction can be calculated as

$$V_0 = \sqrt{\frac{\mu}{p^3}}(1 + e \cos v_0)^2 \Lambda_0' L_0. \tag{3.2}$$

The value $V_0 = -0.5$ m/s is taken as the initial velocity for a circular orbit case. The value of the control coefficient $k_2 = 1.14861$ corresponding to this initial velocity can be calculated using expressions (3.1) and (3.2). It follows from (3.2) that the absolute value V_0 grows with increasing eccentricity at a fixed value of k_2.

Table 1. Parameters of the system

Parameter	Value
L_0 — initial tether length	1000 m
m_1 — mass of the satellite	800 kg
m_2 — mass of the subsatellite	2000 kg
p — semi-latus rectum	687,100 m

To study the influence of the parameter k_1 on the dynamics of the system, a series of simulations using the system of equations (2.7)–(2.8) and the control law (2.6) for various k_1 and eccentricities were carried out. Since the proposed control law provides asymptotic stability, the target position $L = 0$ is achieved at infinite time. Numerical integration of systems of equations (2.7)–(2.8) stopped when the tether reached a finite length $L_k = 0.1$ m. The angle of the true anomaly corresponding to the completion of the calculation is denoted as ν_{end}. The results of numerical calculations are presented in Figs. 2–7. The values T_{max} and T_{min} determine the maximum and minimum value of the tether tension force during tether retrieval, respectively. The values V_{max} and V_{min} determine the maximum and minimum value of the tether retraction velocity. The values Λ_{max} determine the maximum tether length.

Figure 2 shows that, at a small eccentricity, up to $e = 0.3$, the length of the tether does not exceed the initial length $\Lambda_0 = 1$. For orbits with a large eccentricity, the use of the control law leads to the need for additional tether release (Fig. 14). The greater the eccentricity, the longer the tether length is required to implement the control law.

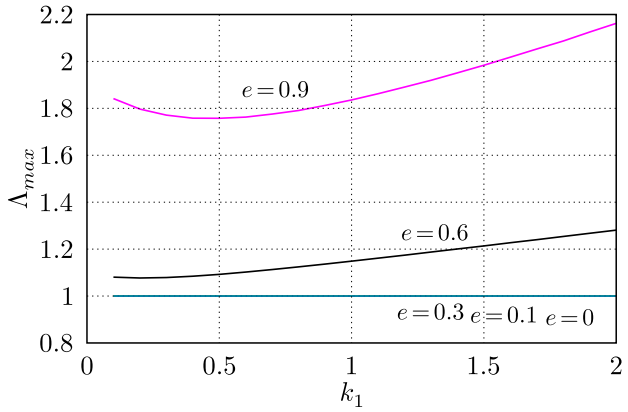

Fig. 2. Changing a parameter Λ_{max}

Figures 3 and 4 demonstrate the maximum and minimum tension force of the tether, which is observed during the tether retrieval operation. The formula (2.9) is used to calculate the tension force. It can be seen from Fig. 3 that an increase in eccentricity leads to an increase in the maximum tension force of the tether, but in all cases the force is quite small and will not lead to tether rupture. An increase in the parameter k_1 of the control law leads to a decrease in the maximum tension force of the tether. According to Fig. 4, for all the considered cases of eccentricities, the minimum tension force for some k_1 may take negative values. These modes of motion are physically unrealizable, since the negative tension force indicates that the tether should push the subsatellite, working as a rod. In fact, when implementing such a control law, the tether slacks. With the growth of k_1 the "slacking" disappears for the case of orbits with a small eccentricity. For eccentricities close to 1, for example, $e = 0.9$ in Fig. 5, slacking cannot be avoided for the considered range of k_1 values. Slacking is typical for the initial states of controlled motion, when the tether is deployed (Fig. 14). The greater the eccentricity, the greater the value k_1 required for physically realizable control.

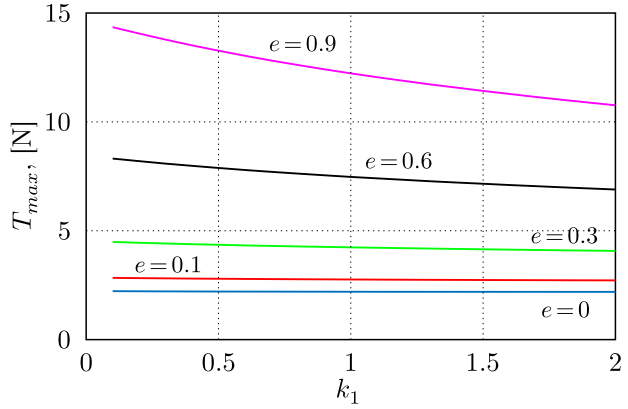

Fig. 3. Changing a parameter T_{max}

It can be seen from Fig. 5 that, with the increase in eccentricity, the value ν_{end} decreases. The dotted line marks the area of a physically unrealizable solution, where the tension force takes negative values (Fig. 4). In other words, less time is required to carry out the operation of the tether retrieval. An interesting feature can be observed: it can be seen from Fig. 8 that, with

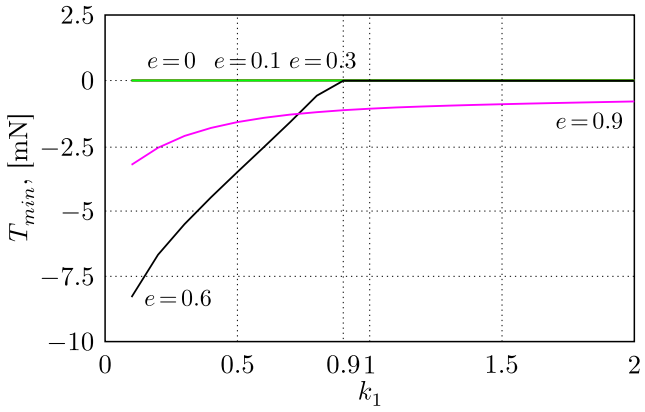

Fig. 4. Changing a parameter T_{min}

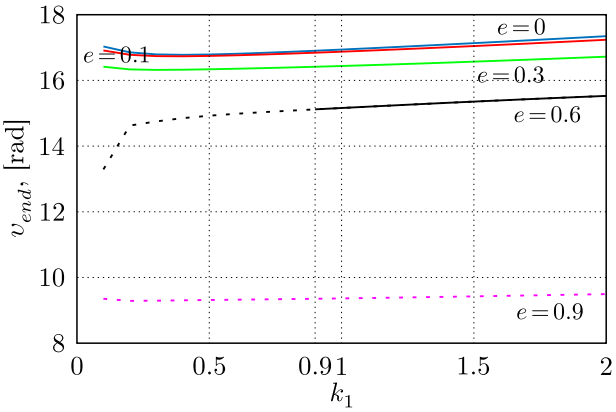

Fig. 5. Changing a parameter ν_{end}

the increase in eccentricity, there is a tendency to reduce the final maneuver execution time. If for eccentricity $e = 0$ we get $\nu_{end} \approx 17$ rad, then for $e = 0.9$ we get $\nu_{end} \approx 9$ rad. Changing the same parameter k_1 has little effect on ν_{end}.

Figure 6 shows that, with increasing eccentricity, the maximum tether retraction velocity $V_{\max}$ also increases. The observed positive values indicate that there is a deployment of the tether, and the tether slacking can be observed (it will be shown below for a particular calculation). Note that the tether deployment is typical for eccentricities $e > 0.3$. The zero value of V_{max} for eccentricities $0 \leqslant e \leqslant 0.3$ indicates that, in these modes, slacking does not occur, but there are moments when the tether is not retrieved and is not deployed. Increasing the parameter k_1 leads to a decrease in the maximum velocity $V_{\max}$.

Figure 7 shows that changing the parameter k_1 does not have any effect on the value V_{min}. With the increase in eccentricity, there is an increase in the minimum tether retractive velocity V_{min}. This confirms the results shown in Fig. 5, which demonstrate a tendency to a decrease in the maneuver time with an increase in e. The large negative velocity of retraction allows the maneuver to be implemented faster.

Let us investigate how the change in the coefficient k_2 affects the motion of the space tether system. To do this, a similar series of calculations were performed by varying the coefficient k_2, at a fixed value of $k_1 = 0.8$. The results are presented in Figs. 8–13. Figure 8 shows that an

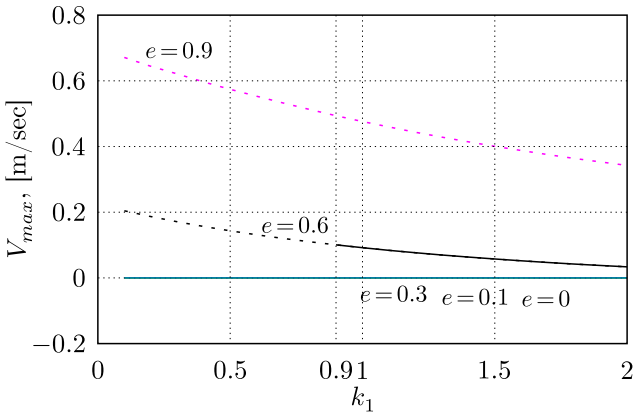

Fig. 6. Changing a parameter V_{max}

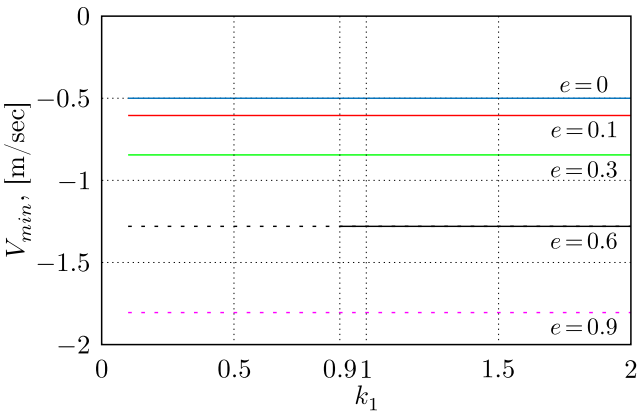

Fig. 7. Changing a parameter V_{min}

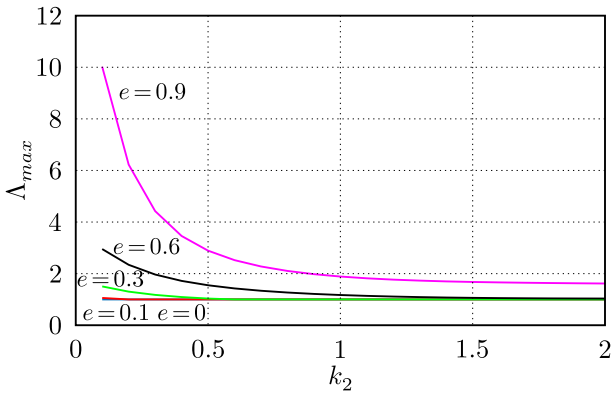

Fig. 8. Changing a parameter Λ_{max}

increase in the parameter k_2 leads to a decrease in the maximum length of the tether. Starting from the value $k_2 \approx 1$, the changes are no longer so significant, and are asymptotic in nature. Here we see a similar trend, there is a need for additional tether deployment with the growth of e to use the control law (2.6).

Figures 9 and 10 demonstrate the maximum and minimum tension force of the tether. Figure 9 shows a trend similar to that seen in Fig. 3. With an increase in eccentricity, the maximum tension force also increases, but at the same time its values will not lead to a break in the tether due to the small value. For example, an average steel tether with a diameter of 2 millimeters has a breaking force near 2000 N. An increase in k_2, for large eccentricities, first leads to a decrease in T_{max}; after the values of $k_2 \approx 1.3$, on the contrary, it increases slightly. For small eccentricities, the picture is generally similar, but the changes are not so significant. For T_{min}, in the range of variation k_2 from 0.45 to 1.65, there is a zero value corresponding to the slacking of the tether. For eccentricity $e = 0.9$, when $0.1 \leqslant k_2 \leqslant 0.45$, negative values of the tension force are observed, which are not physically realized. A similar pattern is observed for all the eccentricities considered, starting from $k_2 \approx 1.7$, where there is a sharp departure of the tension force into the region of negative values. This shows that after the value k_2 the control law cannot be implemented.

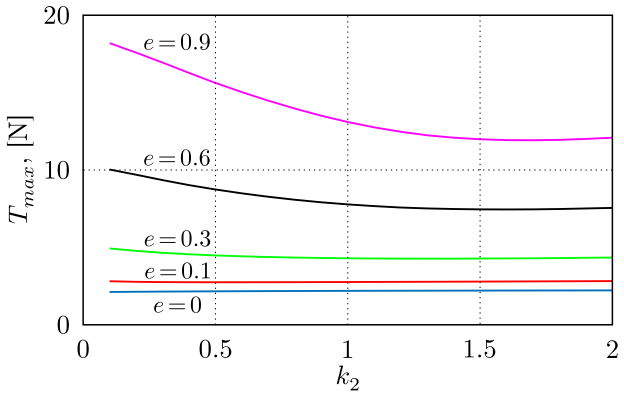

Fig. 9. Changing a parameter T_{max}

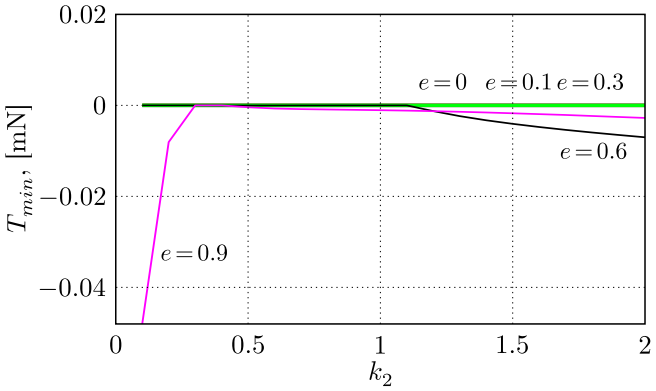

Fig. 10. Changing a parameter T_{min}

Figure 11 demonstrates a picture similar to Fig. 5. With an increase in eccentricity the value of ν_{end} decreases. An increase in the k_2 coefficient leads to a decrease in the ν_{end} value.

Figures 12 and 13 demonstrate the maximum and minimum tether retraction velocity observed during the retrieval process. A similar trend for V_{max} and V_{min} can be noted — an increase in eccentricity leads to an increase in these values. An increase in the coefficient k_2

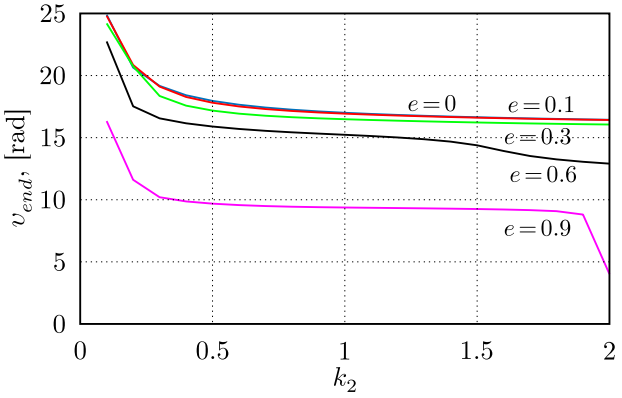

Fig. 11. Changing a parameter ν_{end}

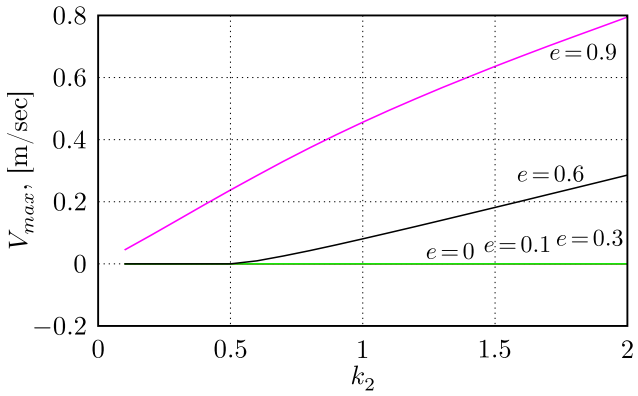

Fig. 12. Changing a parameterV_{max}

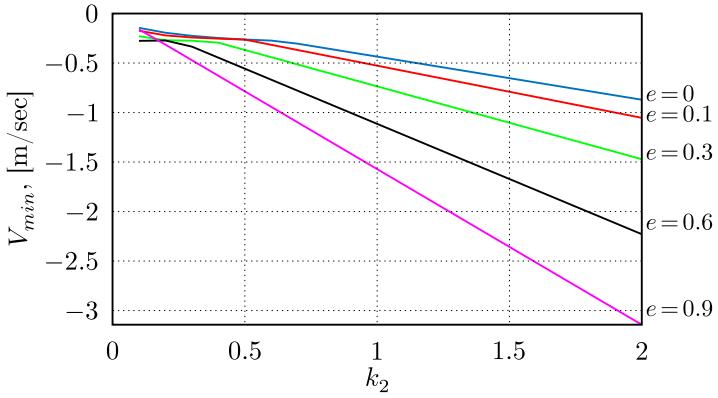

Fig. 13. Changing a parameterV_{min}

leads to an increase in the values V_{max} and V_{min} to. The actual increase in the velocity limits ensures a reduction in the final maneuver time (Fig. 11).

To demonstrate the process of controlled tether retrieval, let us perform a calculation for various eccentricities by choosing fixed control parameters $k_1 = 0.8$ and $k_2 = 1.14861$. The results are presented in Figs. 14–18.

It can be seen from Figs. 14–18 that the developed tether control law (2.6) provides the tether retrieval without winding at the final stage. According to Fig. 16, the tether eventually

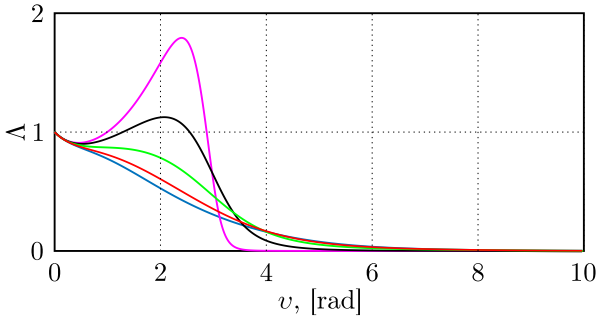

Fig. 14. Changing a parameter Λ

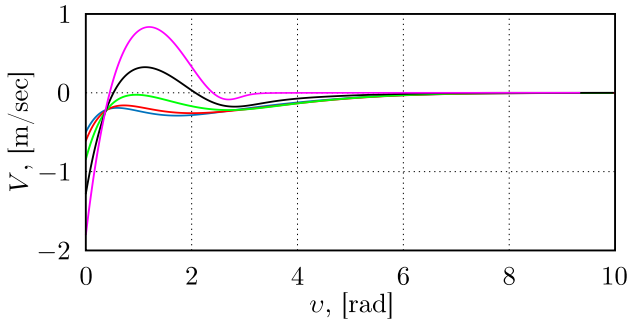

Fig. 15. Changing a parameter V

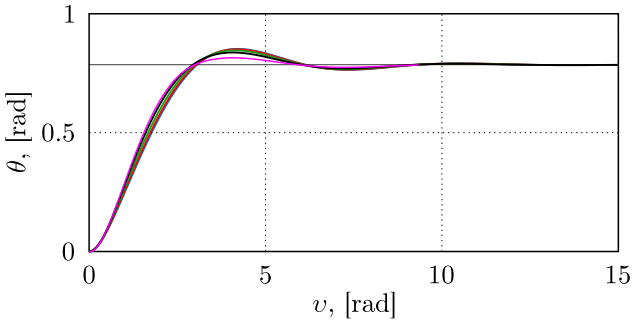

Fig. 16. Changing a parameter θ

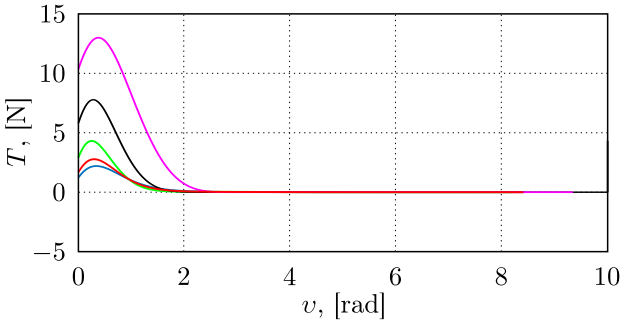

Fig. 17. Changing a parameter T (blue line $e = 0$, red — $e = 0.1$, green — $e = 0.3$, black — $e = 0.6$, purple — $e = 0.9$)

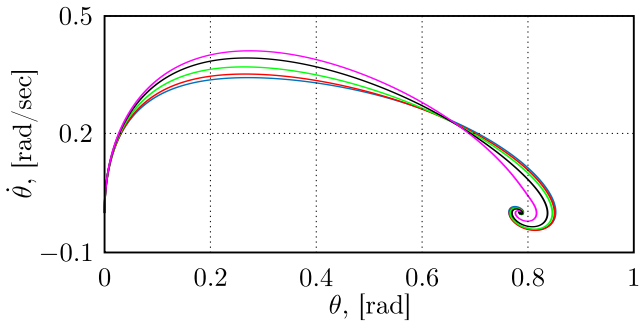

Fig. 18. Phase portrait $\theta(\dot{\theta})$ (blue line $e = 0$, red — $e = 0.1$, green — $e = 0.3$, black — $e = 0.6$, purple — $e = 0.9$)

occupies an angular position $\theta = \frac{\pi}{4}$. The fluctuations in the angle fade by the end of the maneuver. From Fig. 14 it can be seen that, with large eccentricities, the tether first increases its length and deployment occurs. After a while, the tether retraction begins. The tether retrieval operation is successfully completed. From Figure 15 we can see that the tether retrieval velocity monotonically approaches zero as the length of the tether decreases. For large eccentricities, there is a change in the velocity sign. The tether is firstly retracted, then there is a change in the velocity sign, and the deployment begins, then again retraction occurs. This behavior of the tether explains the $\Lambda_{max} > 1$ in Figs. 2 and 8 and the difference between the V_{min} curves for $e = 0.6$ and $e = 0.9$ in Figs. 6 and 12. It should be noted that the proposed law provides the tether retrieval for different eccentricities. It is worth noting that, with large eccentricities, the deployment of the tether is observed at the beginning of the maneuver. This is also confirmed by Fig. 2, where the maximum length of the tether exceeds its initial value. However, this fact does not affect the ability of the law to carry out a given maneuver. The deploying phase of the tether begins to be observed for values $e > 0.3$. For smaller values of eccentricity, the nature of the motion of the system is close to the case of a circular orbit. Figure 17 shows that an increase in the tension force of the tether is observed at the beginning of the maneuver; further, the magnitude of the tension force decreases to almost zero values. For eccentricities greater than $e = 0.6$, a negative value of the tension force is observed, as shown in Figs. 4 and 10. In particular, for $e = 0.6$ the minimum tension force is $T_{min} = -0.55412$ mN, and for $e = 0.9$ the minimum tension force is $T_{min} = -1.2$ mN. In this situation, the tether is slacking, which indicates the impossibility of further use of the control law. From the phase portrait (Fig. 18), the same behavior of the system's phase trajectories is observed.

From Figures 14–18, it can be concluded that the proposed control allows the tether to be retrieved both in circular and elliptical orbits with a large eccentricity. For highly elliptical orbits, it will be necessary to lay a reserve of tether length, to ensure the initial deployment of the tether, this reserve can be estimated from the results of numerical simulations. The main factors influencing the choice of parameters of the control law are the initial velocity of the tether retraction and the minimum tension force in the tether.

4. Conclusion

This study considers a variable length space tether system. A novel nonlinear tether length control law that ensures the tether retraction in an elliptical orbit without the tether winding at the final stage of the tether retrieval maneuver is proposed. The asymptotic stability of controlled

motion in elliptical orbits is proved using the Lyapunov theory. The influence of the parameters of the control law and the eccentricity of the orbit on the tether length and the tension force is investigated by a series of numerical simulations. The results of numerical simulations confirm that the control law obtained solves the problem of the tether retrieval in elliptical orbits.

Since the developed control law provides asymptotic stability of the motion, the tether cannot be fully drawn into the satellite in finite time. In this regard, it is advisable to equip the satellite with robot manipulators capable of capturing a tethered subsatellite at a short distance from it. The results of this study can be applied in preparing the tether-assisted space debris removal missions and in performing operations involving tether retrieval.

Conflict of interest

The authors declare that they have no conflict of interest.

References

[1] Cartmell, M. P. and McKenzie, D. J., A Review of Space Tether Research, *Prog. Aerosp. Sci.,* 2008, vol. 44, no. 1, pp. 1–21.

[2] Huang, P., Zhang, F., Chen, L., Meng, Z., Zhang, Y., Liu, Z., and Hu, Y., A Review of Space Tether in New Applications, *Nonlinear Dyn.,* 2018, vol. 94, no. 1, pp. 1–19.

[3] Chen, Y., Huang, R., He, L., Ren, X., and Zheng, D., Dynamical Modelling and Control of Space Tethers: A Review of Space Tether Research, *Nonlinear Dyn.,* 2014, vol. 77, no. 4, pp. 1077–1099.

[4] Yu, B. S., Wen, H., and Jin, D. P., Review of Deployment Technology for Tethered Satellite Systems, *Acta Mech. Sin.,* 2018, vol. 34, no. 4, pp. 754–768.

[5] Bekey, I. and Penzo, P. A., Tether Propulsion, *Aerosp. Am.,* 1986, vol. 24, no. 7, pp. 40–43.

[6] Pikalov, R. S., Strategy for the Realization of Soft Docking with Space Debris by Using a Tether System, *J. Phys. Conf. Ser.,* 2019, vol. 1368, no. 4, 042026, 5 pp.

[7] Trushlyakov, V. I., Yudintsev, V. V., and Onishchuk, S. Yu., Risks of Docking and Nulling of the Kinetic Moment of an Uncooperative Large-Sized Space Debris, *J. Space Saf. Eng.,* 2022, vol. 9, no. 4, pp. 523–527.

[8] Mayorova, V. I., Shcheglov, G. A., and Stognii, M. V., Analysis of the Space Debris Objects Nozzle Capture Dynamic Processed by a Telescopic Robotic Arm, *Acta Astronaut.,* 2021, vol. 187, pp. 259–270.

[9] Sizov, D. A. and Aslanov, V. S., Space Debris Removal with Harpoon Assistance: Choice of Parameters and Optimization, *J. Guid. Control Dyn.,* 2020, vol. 44, no. 4, pp. 767–778.

[10] Barnes, C. M. and Botta, E. M., A Quality Index for Net-Based Capture of Space Debris, *Acta Astronaut.,* 2020, vol. 176, pp. 455–463.

[11] Xu, D. M., Misra A. K., and Modi, V. J., Thruster-Augmented Active Control of a Tethered Subsatellite System during Its Retrieval, *J. Guid. Control Dyn.,* 1986, vol. 9, no. 6, pp. 663–672.

[12] Netzer, E. and Kane, T. R., Deployment and Retrieval Optimization of a Tethered Satellite System, *J. Guid. Control Dyn.,* 1993, vol. 16, no. 6, pp. 1085–1091.

[13] Yingying, L., Jun, Z., and Huanlong, C., Variable Structure Control for Tethered Satellite Fast Deployment and Retrieval, in *Future Control and Automation,* W. Deng (Ed.), Lect. Notes Electr. Eng., vol. 172, Berlin: Springer, 2012, pp. 157–164.

[14] Fujii, H. and Ishijima, S., Mission-Function Control for Slew Maneuver of a Flexible Space Structure, *J. Guid. Control Dyn.,* 1989, vol. 12, no. 6, pp. 858–865.

[15] Kokubun, K. and Fujii, H. A., Deployment/Retrieval Control of a Tethered Subsatellite under Effect of Tether Elasticity, *J. Guid. Control Dyn.,* 1996, vol. 19, no. 1, pp. 84–90.

[16] Pradeep, S., Tension Control of Tethered Satellites, in *AIAA/AAS Astrodynamics Specialsist Conference and Exhibit (Boston, Mass., 1998),* pp. 44–75.

[17] Kumar, K., Pradeep, S., and Vidya, G., Optimization of Control Gains for Three Dimensional Retrieval Dynamics of Tethered Satellites, in *Proc. of the 7th AIAA/USAF/NASA/ISSMO Symp. on Multidisciplinary Analysis and Optimization (St. Louis, Mo., 1998),* pp. 49–78.

[18] Djebli, A., Pascal, M., and El Bakkali, L., Laws of Deployment/Retrieval in Tether Connected Satellites Systems, *Acta Astronaut.,* 1999, vol. 45, no. 2, pp. 61–73.

[19] Djebli, A., El Bakkali, L., and Pascal, M., On Fast Retrieval Laws for Tethered Satellite Systems, *Acta Astronaut.,* 2002, vol. 50, no. 8, pp. 461–470.

[20] Sun, G. and Zhu, Z. H., Fractional Order Tension Control for Stable and Fast Tethered Satellite Retrieval, *Acta Astronaut.,* 2014, vol. 104, no. 1, pp. 304–312.

[21] Chernous'ko, F. L., Dynamics of the Retrieval of a Tethered Space System, *J. Appl. Math. Mech.,* 1995, vol. 59, no. 2, pp. 165–173; see also: *Prikl. Mat. Mekh.,* 1995, vol. 59, no. 2, pp. 179–187.

[22] Kalashnikov, L. M., Malyshev, G. V., and Svotin, A. P., The Control of Two-Module Space Rope System Rolling, *Probl. Upr.,* 2003, no. 4, pp. 63–66 (Russian).

[23] Zabolotnov, Yu. M., Control of the Deployment of an Orbital Tether System That Consists of Two Small Spacecraft, *Cosmic Research,* 2017, vol. 55, no. 3, pp. 224–233; see also: *Kosmicheskie Issledovaniya,* 2017, vol. 55, no. 3, pp. 236–246.

[24] Aslanov, V. S. and Pikalov, R. S. Rendezvous of Non-Cooperative Spacecraft and Tug Using a Tether System, *Eng. Lett.,* 2017, vol. 25, no. 2, pp. 142–146.

[25] Zhong, R. and Zhu, Z. H., Dynamic Analysis of Deployment and Retrieval of Tethered Satellites Using a Hybrid Hinged-Rod Tether Model, *IJALS,* 2011, vol. 1, no. 2, pp. 239–259.

[26] Zhang, F. and Huang, P., Segmented Control for Retrieval of Space Debris after Captured by Tethered Space Robot, in *IEEE/RSJ Internat. Conf. on Intelligent Robots and Systems (Hamburg, Germany, 2015),* pp. 5454–5459.

[27] Zhang, F. and Huang, P., A Novel Underactuated Control Scheme for Deployment/Retrieval of Space Tethered System, *Nonlinear Dyn.,* 2019, vol. 95, no. 4, pp. 3465–3476.

[28] Vadali, S. R., Feedback Tether Deployment and Retrieval, *J. Guid. Control Dyn.,* 1991, vol. 14, no. 2, pp. 469–470.

[29] Kim, E. and Vadali, S. R., Nonlinear Feedback Deployment and Retrieval of Tethered Satellite Systems, *J. Guid. Control Dyn.,* 1992, vol. 15, no. 1, pp. 28–34.

[30] Ma, Z. and Sun, G., Full-Order Sliding Mode Control for Deployment/Retrieval of Space Tether System, in *IEEE Internat. Conf. on Systems, Man, and Cybernetics (SMC, Budapest, Hungary, Oct 2016),* pp. 407–412.

[31] Kang, J. and Zhu, Z. H., Hamiltonian Formulation and Energy-Based Control for Space Tethered System Deployment and Retrieval, *Trans. Can. Soc. Mech. Eng.,* 2019, vol. 43, no. 4, pp. 463–470.

[32] Fujii, H. A. and Kojima, H., Optimal Trajectory Analysis for Deployment/Retrieval of Tethered Subsatellite Using Metric, *J. Guid. Control Dyn.,* 2003, vol. 26, no. 1, pp. 177–179.

[33] Lakso, J. and Coverstone, V., Optimal Tether Deployment/Retrieval Trajectories Using Direct Collocation, in *Astrodynamics Specialist Conf. (Denver, Colo., Aug 2000),* pp. 43–49.

[34] Steindl, A., Steiner, W., and Troger, H., Optimal Control of Retrieval of a Tethered Subsatellite, in *IUTAM Symp. on Chaotic Dynamics and Control of Systems and Processes in Mechanics (Dordrecht, The Netherlands, 2005),* pp. 441–450.

[35] Steindl, A. and Troger, H., Optimal Control of Deployment of a Tethered Subsatellite, *Nonlinear Dyn.,* 2003, vol. 31, no. 3, pp. 257–274.

[36] Steindl, A., Optimal Control of the Deployment (and Retrieval) of a Tethered Satellite under Small Initial Disturbances, *Meccanica,* 2014, vol. 49, no. 8, pp. 1879–1885.

[37] Ohtsuka, T., Nonlinear Optimal Feedback Control for Deployment/Retrieval of a Tethered Satellite, *Trans. Jpn. Soc. Aeronaut. Space Sci.,* 2001, vol. 43, no. 142, pp. 165–173.

[38] Williams, P., Deployment/Retrieval Optimization for Flexible Tethered Satellite Systems, *Nonlinear Dyn.,* 2008, vol. 52, no. 1, pp. 159–179.

[39] Yu, B. S. and Jin, D. P., Deployment and Retrieval of Tethered Satellite System under J2 Perturbation and Heating Effect, *Acta Astronaut.,* 2010, vol. 67, nos. 7–8, pp. 845–853.

[40] Razoumny, Yu. N., Kupreev, S. A., and Misra, A. K., The Research Method of Controlled Movement Dynamics of Tether System, in *Proc. of the 1st IAA/AAS SciTech Forum on Space Flight Mechanics and Space Structures and Materials (Moscow, Russia, Nov 2018),* Yu. N. Razoumny, F. Graziani, A. D. Guerman, J.-M. Contant (Eds.), Adv. Astronaut. Sci., vol. 170, San Diego, Calif.: Univelt, 2020, pp. 417–431.

[41] Pang, Z., Wen, H., Rui, X., and Du, Z., Nonlinear Resonant Analysis of Space Tethered Satellite System in Elliptical Orbits, *Acta Astronaut.,* 2021, vol. 182, pp. 264–273.

[42] Souza dos Santos, D. P., Da Rocha e Brito de Aguiã Morant, S. A., Guerman, A. D., and Burov, A. A., Stability Solutions of a Dumbbell-Like System in an Elliptical Orbit, *J. Phys. Conf. Ser.,* 2015, vol. 641, no. 1, 012004, 7 pp.

[43] Wang, C. Wang, P. Li, A., and Guo, Y., Deployment of Tethered Satellites in Low-Eccentricity Orbits Using Adaptive Sliding Mode Control, *J. Aerosp. Eng.,* 2017, vol. 30, no. 6, 04017077.

[44] Malkin, I. G., *Theory of Stability of Motion,* Washington, D.C.: U.S. Atomic Energy Commission, 1952.